iScience

CellPress
OPEN ACCESS

Article

Regional homogeneity as a marker of sensory cortex dysmaturity in preterm infants

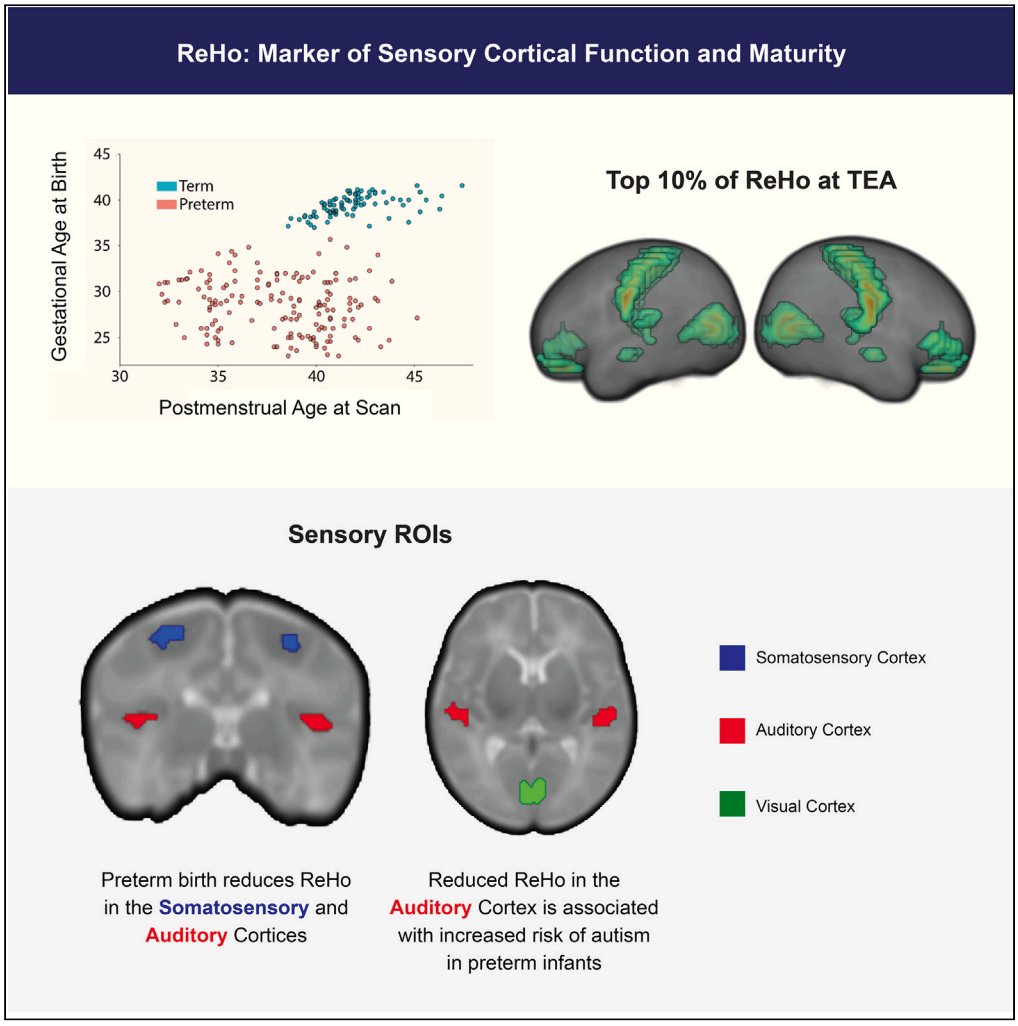

Srikanth R. Damera, Josepheen De Asis-Cruz, Kevin M. Cook, ..., Sudeepta Basu, Nickie Andescavage, Catherine Limperopoulos

climpero@childrensnational.org

Highlights

Regional homogeneity (ReHo) reflects the maturity of cortical areas

Preterm birth differentially reduces ReHo in the sensory cortices

Sensory cortices mature at different rates between 32 and 48 weeks gestational age

Reduced ReHo in the auditory cortex predicts increased risk of autism

Damera et al., iScience 27, 109662
May 17, 2024
https://doi.org/10.1016/j.isci.2024.109662

iScience

CellPress
OPEN ACCESS

Article

Regional homogeneity as a marker of sensory cortex dysmaturity in preterm infants

Srikanth R. Damera,[1] Josepheen De Asis-Cruz,[1] Kevin M. Cook,[1] Kushal Kapse,[1] Emma Spoehr,[1] Jon Murnick,[1] Sudeepta Basu,[1] Nickie Andescavage,[1] and Catherine Limperopoulos[1,2,*]

SUMMARY

Atypical perinatal sensory experience in preterm infants is thought to increase their risk of neurodevelopmental disabilities by altering the development of the sensory cortices. Here, we used resting-state fMRI data from preterm and term-born infants scanned between 32 and 48 weeks post-menstrual age to assess the effect of early ex-utero exposure on sensory cortex development. Specifically, we utilized a measure of local correlated-ness called regional homogeneity (ReHo). First, we demonstrated that the brain-wide distribution of ReHo mirrors the known gradient of cortical maturation. Next, we showed that preterm birth differentially reduces ReHo across the primary sensory cortices. Finally, exploratory analyses showed that the reduction of ReHo in the primary auditory cortex of preterm infants is related to increased risk of autism at 18 months. In sum, we show that local connectivity within sensory cortices has different developmental trajectories, is differentially affected by preterm birth, and may be associated with later neurodevelopment.

INTRODUCTION

The developing brain is characterized by a series of critical periods,[1] or periods of heightened plasticity, during which environmental influences exert lasting effects on developing cortical function. In contrast, experiences outside of critical periods have a much more limited effect on cortical function.[2–4] Sensory cortices are among the first brain areas to mature and are thought to help organize the higher-order areas that emerge later in development.[5] In humans, certain critical periods for primary sensory cortices are thought to open *in utero*.[6,7] For infants born preterm, these critical periods occur in a significantly altered *ex utero* sensory environment. Thus, these early atypical sensory experiences may have lasting impacts on the development of individual sensory cortices as well as on overall brain organization and function. Such altered sensory processing is thought to underlie several neurodevelopmental disabilities, including autism.[8–10] Understanding how preterm birth and postnatal experience shape sensory cortices may shed light on the known risk of neurodevelopmental disabilities in children born preterm.[10–12]

While the biologic underpinnings of neurodevelopmental disabilities in children born preterm are not fully elucidated, magnetic resonance imaging (MRI) techniques have identified differences in sensory cortices between full-term and preterm infants. Functional MRI (fMRI) studies have shown that despite similarities in the whole-brain network architecture at term-equivalent age (TEA), preterm sensory networks are marked by reduced long-range connectivity to other subcortical and cortical areas.[13–22] Still, typical development of a sensory area is determined by both its long-range connectivity and its local functional properties.[23] To date, the only studies examining the local development of cortical areas have looked at structural features (e.g., synaptogenesis),[5,24–29] and have shown that they mature faster in sensory areas relative to the rest of the brain and are diminished by preterm birth. However, it is still unclear how local functional properties of sensory cortices develop during the perinatal period and are affected by preterm birth.

Local connectivity methods can interrogate the functional profile of cortical areas in the absence of stimuli. One such method is regional homogeneity (ReHo) analysis.[30,31] ReHo is the Kendall coefficient of concordance between the resting-state fMRI (rsFMRI) time series of a single voxel and those of its nearest neighbors. Prior work has shown that it has high test-retest reliability with only 5 min of rsFMRI data.[32] Furthermore, it has been linked to changes in local excitability and inhibition,[33,34] sensory learning,[30,35–37] and neurodevelopmental disability.[34,38,39] Thus, ReHo may be a promising marker of sensory cortex dysmaturity.

In the current work, we conducted a case-control study in which we used ReHo to interrogate functional changes in the sensory cortices of preterm infants and explored how these changes were associated with neurodevelopmental outcomes. Overall, we hypothesized that preterm birth would lead to altered maturation of sensory cortices in preterm infants and that this effect may vary across sensory cortices. To assess this overarching objective, we first examined if the distribution of ReHo across cortex at TEA mirrored the known gradient of structural cortical maturation. We then tested the impact of preterm birth on ReHo across the sensory cortices at TEA. Next, we examined the

[1]Developing Brain Institute, Children's National, 111 Michigan Avenue NW, Washington, DC 20010, USA
[2]Lead contact
*Correspondence: climpero@childrensnational.org
https://doi.org/10.1016/j.isci.2024.109662

Table 1. Subject clinical characteristics

	Term infants (n = 86)	Preterm infants (n = 133)
Birth gestational age ($\mu \pm \sigma$ weeks)	39.5 ± 1.1	28.2 ± 2.9
Post-menstrual age at scan ($\mu \pm \sigma$ weeks)	41.9 ± 1.8	Scanned before TEA (n = 57)[1]: 34.5 ± 1.2 Scanned after TEA (n = 109): 40.1 ± 1.9
Birth weight ($\mu \pm \sigma$ grams)	3307.4 ± 425.0	1062.3 ± 452.1
Sex (n)	46 M	61 M
Kidokoro score ($\mu \pm \sigma$ score)	–	3.2 ± 1.9
BPD present (n)	–	40
NEC present (n)	–	41
PDA present (n)	–	67
PNS received (n)	–	72
18-month MCHAT recorded (n)	–	38
18-month MCHAT scores ($\mu \pm \sigma$)		1.9 ± 3.3

Clinical characteristics of study subjects. M, male; BPD, bronchopulmonary dysplasia; NEC, necrotizing enterocolitis; PDA, patent ductus arteriosus; PNS, prenatal steroids.[1] 32 subjects were scanned both before and after TEA.

developmental trajectory of ReHo in preterm infants during the third trimester. Finally, we performed an exploratory analysis examining the relationship between ReHo and future autism risk in preterm infants.

RESULTS

Clinical characteristics of the study cohort

In total, we analyzed data from 86 term-born infants ($\mu_{GA} \pm \sigma_{GA}$ = 39.5 ± 1.1; $\mu \pm \sigma_{CA}$ = 41.9 ± 1.8 weeks; 46 males) and 133 preterm infants. Of the 133 preterm infants, 109 ($\mu_{GA} \pm \sigma_{GA}$ = 28.2 ± 2.9; $\mu_{PMA} \pm \sigma_{PMA}$ = 40.1 ± 1.9 weeks; 49 males) were scanned at TEA (≥37 weeks post-menstrual age [PMA]) and 57 ($\mu_{GA} \pm \sigma_{GA}$ = 29.3 ± 2.7; $\mu_{PMA} \pm \sigma_{PMA}$ = 34.5 ± 1.2 weeks; 28 males) were scanned before TEA (Table 1). Thirty-two preterm infants were scanned longitudinally and contributed to both pre- and post-TEA datasets.

Distribution of ReHo across cortex at TEA and defining sensory ROIs

First, we examined the distribution of ReHo across the cortex at TEA by identifying voxels where the average ReHo across both term-born and preterm infants was different from 0 (voxel-wise p-value <0.001; Figure 1A). We further examined the spatial distribution of ReHo by plotting the top 10% of significant positive voxels across cortex. This demonstrated that bilateral primary sensory areas as well as orbitofrontal cortex, hippocampus, and thalamus show elevated synchronous activity (Figure 1B). Of note, orbitofrontal cluster contains several voxels with a low signal-to-noise ratio (Figure S1). We then used this map to generate equally sized regions of interest (ROIs) in each of the primary sensory areas (Figure 1C; see STAR Methods).

The impact of preterm birth on ReHo across sensory cortices at TEA

Next, we tested how preterm birth affected ReHo in each of the three sensory cortices at TEA after correcting for their PMA when scanned (Equation 1; Figure 2; Table S1). This showed that preterm birth reduced ReHo in the somatosensory (t_{189} = −6.07, p_{HC} = 2.079e−8) and auditory (t_{188} = −2.28, p_{HC} = 0.047) but not visual (t_{188} = −0.59, p_{HC} = 0.556) cortices.

We also tested if the effect of preterm birth on the somatosensory and auditory cortex was specific to these areas or reflected a general effect of preterm birth on the developing brain. Our results (Figure S2) show that the reduction in ReHo due to preterm birth in the somatosensory ($p < 0.001$) and auditory ($p = 0.05$) ROIs is unlikely to reflect a general effect of preterm birth on the developing brain.

The differential effect of preterm birth on ReHo across the sensory cortices at TEA

We then explicitly tested if preterm birth differentially affected sensory areas (Equation 2). This revealed a significant interaction between preterm birth and sensory ROIs ($F_{2,380}$ = 4.39, p = 0.013). Post hoc testing revealed that this interaction was due to a significantly greater effect of preterm birth on the somatosensory cortex compared to the auditory (t_{383} = 2.55, p_{HC} = 0.022) and visual (t_{383} = 2.58, p_{HC} = 0.021) cortices. There was no significant difference between the auditory and visual cortex (t_{382} = 0.03, p_{HC} = 0.98).

The effect ofbBirth GA and PMA on the developmental trajectory of ReHo across the sensory cortices of preterm infants

We tested the effects of PMA at scan and birth gestational age (GA) on ReHo in each of the sensory cortices of preterm infants while controlling for several clinical covariates (Equation 3; Figure 3A; Table S2). This showed a positive effect of PMA in the somatosensory

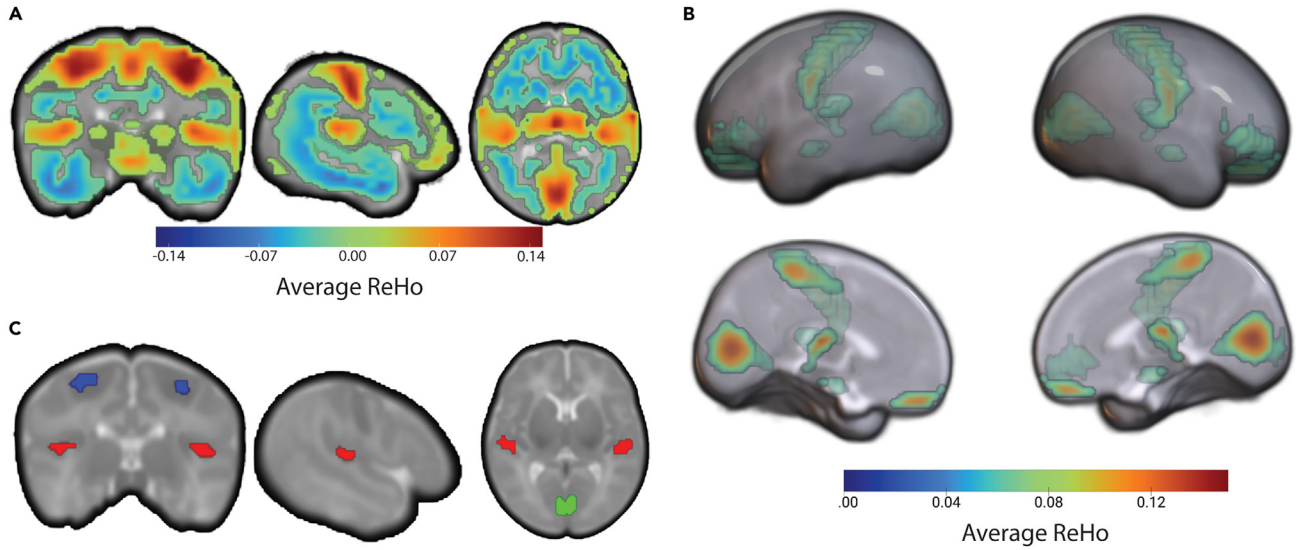

Figure 1. Defining regions of interest (ROIs) in the primary sensory cortices

(A) Shows the voxel where ReHo is significantly (voxel-wise $p < 0.001$) different from 0.

(B) Shows the spatial distribution of the top 10% of significant ReHo voxels in (A). Color represents the average ReHo across both term and preterm infants at term-equivalent age (TEA).

(C) Shows the final bilateral primary sensory ROIs. Blue, green, and red, correspond to primary somatosensory, visual, and auditory ROIs, respectively. See also Figure S1.

(t_{154} = 5.97, p_{HC} = 3.22e−8), visual (t_{153} = 13.02, p_{HC} = 4.35e−26), and auditory (t_{153} = 4.78, p_{HC} = 4.09e−6) ROIs. However, there was no significant effect of birth GA on ReHo in this group for any brain area (Figure 3B).

The differential effect of PMA on the developmental trajectory ReHo across the sensory cortices of preterm infants

We then explicitly tested if PMA differentially affected sensory areas in preterm infants (Equation 4). This revealed a significant interaction between PMA and sensory ROI ($F_{2,345}$ = 41.14, $p < 0.0001$). Post hoc testing revealed that this interaction was due to a significantly greater effect of PMA on the visual cortex compared to the auditory (t_{357} = 8.78, $p_{HC} < 0.0001$) and somatosensory (t_{358} = 6.38, $p_{HC} < 0.0001$) cortices as well as a significantly greater effect on the somatosensory than auditory cortex (t_{358} = 2.42, p_{HC} = 0.016).

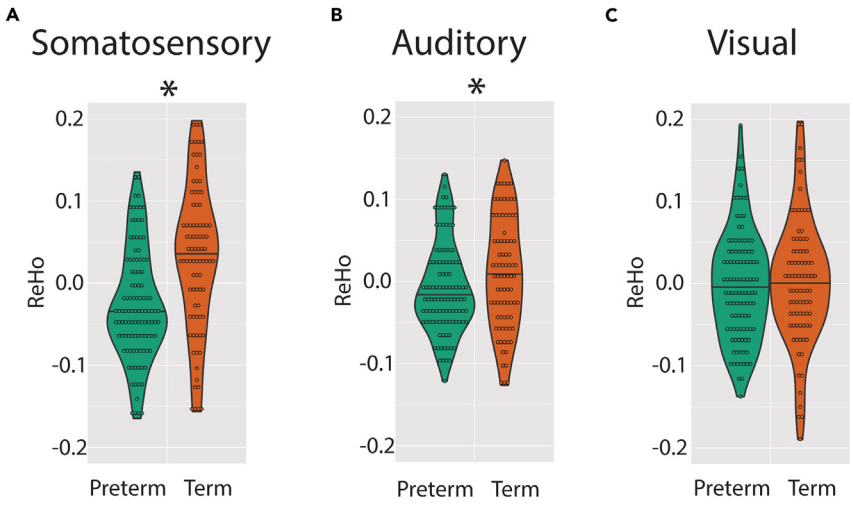

Figure 2. Preterm birth differentially alters ReHo across sensory cortices at TEA

(A–C) Partial dependence plot shows the effect of preterm birth on ReHo at TEA across the three sensory cortices. * Indicates $p_{HC} < 0.05$. See also Figure S2.

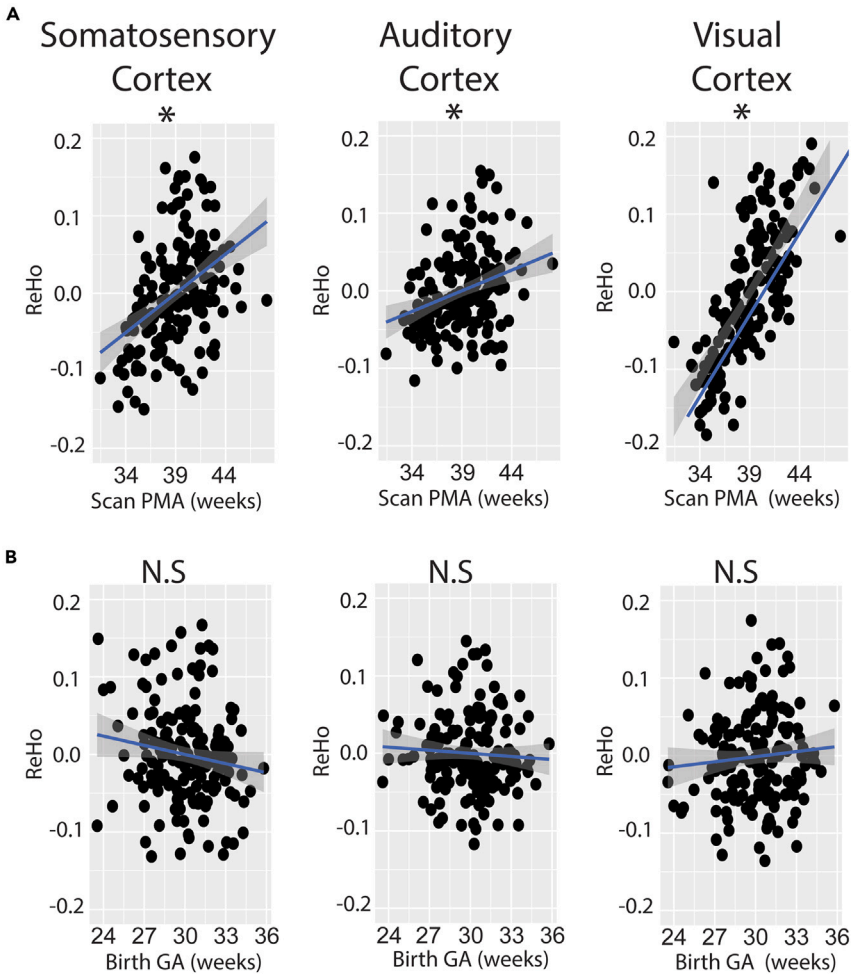

Figure 3. ReHo increases with PMA in the sensory cortices of preterm infants

(A and C) Partial dependence plots which show the effect of scan PMA and birth GA on ReHo in preterm infants across the three sensory cortices. PMA and birth GA are displayed in terms of weeks, but plotted data reflect residuals after accounting for the other variables in the model. * Indicates $p_{HC} < 0.05$.

ReHo in the auditory cortex is negatively associated with MCHAT scores at 18 months in preterm infants

Finally, we performed an exploratory analysis to test the hypothesis that ReHo was negatively associated with increased autism risk as measured by Modified Checklist for Autism in Toddlers (MCHAT) scores at 18 months Equation 5; Table 2). This revealed a negative relationship between ReHo in the auditory cortex and MCHAT scores ($\beta_{MCHAT} = -0.38$, $t_{42} = -2.45$, $p = 0.023$), but no significant relationship in either the somatosensory or visual cortices. It also revealed a positive association between bronchopulmonary dysplasia and MCHAT scores.

DISCUSSION

In the current study, we used ReHo to understand the effects of preterm birth, age, and experience on the developing sensory cortices. First, we showed that the distribution of ReHo is highest in the sensory cortices, mirroring what is known about the maturation of the cerebral cortex. Then we showed that preterm birth reduces ReHo in the somatosensory and auditory but not the visual cortex of preterm infants at TEA. Furthermore, preterm infants demonstrated increasing ReHo with advancing PMA across all sensory areas. However, this rate of maturation is unequal across sensory cortices. Finally, we demonstrated that reduced ReHo in the auditory cortex of preterm infants is associated with increased autism risk scores at 18 months. By jointly studying human primary sensory areas *in vivo* using fMRI, we showed that preterm infants have different developmental trajectories and are differentially sensitive to the effects of preterm birth.

For both term and preterm infants at TEA, the distribution of ReHo is highest in the sensory cortices. Classical studies show that cortical circuits in sensory areas mature faster, as measured by levels of synaptogenesis, than frontal or association areas.[5,25]

Table 2. Association between MCHAT scores and ReHo in the sensory cortices of preterm infants

	Somatosensory cortex			Visual cortex			Auditory cortex		
Predictors	*std.*	*t*	$p_{uncorrected}$	*std.*	*t*	$p_{uncorrected}$	*std.*	*t*	$p_{uncorrected}$
(Intercept)	−0.43	−1.40	1.76e−01	−0.43	−1.46	1.6e−01	−0.38	−2.04	5.37e−02
ReHo	−0.10	−0.60	5.56e−01	−0.04	−0.21	8.38e−01	−0.38[a]	−2.45	2.33e−02
PMA	0.24	1.46	1.60e−01	0.26	1.43	1.67e−01	0.32[a]	2.14	4.41e−02
NEC (YES)	0.57	1.70	1.05e−01	0.56	1.55	1.37e−01	0.59	1.95	6.43e−02
BPD (YES)	1.22[b]	3.03	6.32e−03	1.24[b]	3.04	6.29e−03	0.93[a]	2.46	2.29e−02
$N_{Preterm}$	26 subj			26 subj			26 subj		
Observations	26			26			26		
R^2	0.463			0.455			0.575		

[a] $p < 0.05$.
[b] $p < 0.01$.

Furthermore, recent structural MRI studies show that microstructural features such as fractional anisotropy, myelination, and neurite density are greatest in the sensory cortices at TEA.[28,29,40] Most prior studies of cortical *functional* maturity have focused on the development of long-range connections between the sensory cortices and other brain areas.[13,16,20,22,41] In contrast, here we show, for the first time, that ReHo may be a local marker of cortical functional maturation. Still, the exact drivers of ReHo are unclear. One possibility is that ReHo reflects the local synchronization of neuronal activity. A major source of local synchronous activity that increases with development throughout the third trimester and beyond is gamma oscillatory activity.[42–44] Gamma oscillations reflect synchronization of local cortical patches through rhythmic perisomatic inhibition of pyramidal neurons by parvalbumin-positive interneurons. Importantly, increased inhibitory tone and the emergence of gamma oscillatory activity is thought to mark the opening of critical periods in cortical circuits.[1,45] Furthermore, it was shown that reducing the inhibition of parvalbumin interneurons also reduces ReHo.[34] Together, this raises the exciting possibility that ReHo may be used as a marker for critical periods during which sensory experiences have long-term neurodevelopmental consequences. However, future studies are needed to distinguish this association from the wide array of other possible mechanisms underlying ReHo.

We do note that in addition to the sensory cortices, we also identify an area of increased ReHo in the orbitofrontal cortex. Despite the orbitofrontal cortex being a low signal-to-noise ratio region (Figure S1), we posit these differences reflect biologic differences in the developing brain. The frontal cortex, a structurally and functionally diverse area, is known to mature at different rates for distinct subregions; indeed, classical histology studies show that the development of the sensory cortex prior to the frontal cortex relied on tissue from isocortical areas such as the middle frontal gyrus. In contrast, the development of the orbitofrontal cortex has not been well studied. Recent MRI studies show parallel developmental timelines of orbitofrontal and sensory areas but not prefrontal ones.[28,29] For instance, Dimitrova et al.[28] showed that dendritic branching, measured by orientation dispersion index, was diminished in sensory and orbitofrontal areas of preterm relative to term infants. Batalle et al.[29] showed that markers of myelination increased with PMA in sensory and orbitofrontal areas but not prefrontal areas more generally. Similarly, our results show that ReHo is not uniformly increased across prefrontal cortex but is restricted to orbitofrontal cortex with peak ReHo in the rectus gyrus. It has been shown that this paralimbic region of cortex has both different cytoarchitectonics,[46,47] connectivity,[48] and potentially developmental trajectory[29,49] than other areas of frontal cortex. Our results are consistent with these findings.

Cortical circuit maturation is a combination of experience-dependent and independent factors. Here, we show that a major experience, preterm birth, reduces ReHo in the somatosensory and auditory cortices. An important sequalae of preterm birth is early exposure to the *ex utero* sensory environment, which may alter the developmental trajectory of sensory cortices. Indeed, prior work suggests auditory experience in the neonatal intensive care unit can alter structural and functional maturation of auditory processing pathways and predict neurodevelopmental outcomes in preterm infants.[50–52] Similarly, sensory experience may alter somatosensory activation and connectivity in preterm infants.[53] Our results suggest that sensory experience may delay cortical maturation in the auditory and somatosensory cortex. This is consistent with prior work showing that preterm birth delays maturation of local microstructural features (e.g., cortical thickness, neurite density, etc.) and long-range functional connectivity.[13,22,54–57] Still, other work suggests that postnatal sensory experience in preterm infants accelerates maturation of sensory cortices[18,58–61]—potentially through mechanisms like the maturation of inhibitory circuitry.[62] This discrepancy may arise due to limitations in the ability to precisely quantify the type and amount of postnatal sensory experience received by preterm infants in the face of other conditions (e.g., comorbidities, nutrition, etc.) that are highly correlated with prematurity. Importantly, either delayed or atypically accelerated cortical maturation may be maladaptive given the highly complex temporally regulated interactions between systems in the developing brain.[63,64] In sum, it is likely that the type, degree, duration, and timing of discrete sensory inputs delivered may promote or impair the development of cortical circuits in preterm infants, depending on the developmental window of exposure. Future studies should explicitly test how the amount, quality, and timing of sensory stimuli affect cortical circuit maturation.

Interestingly, unlike the somatosensory and auditory cortices, we also show that ReHo in the visual cortex is unaffected by preterm birth, suggesting distinct developmental trajectories for each of the sensory cortices. Despite postmortem and structural MRI studies which highlight the earlier development of sensory versus higher-order cortical areas,[5,24,28] this work explicitly compares the maturation of human sensory cortices to each other *in vivo*. We also show that sensory cortices of preterm infants are differentially affected by PMA. Just as cortical circuit maturation is a combination of experience-dependent and independent factors, PMA reflects both such factors. Teasing apart which factors are altered in individual sensory cortices will require explicit control over the type and amount of sensory experience received by preterm infants, which may be limited in the clinical setting. Despite this challenge, understanding how experience-dependent factors shape the developmental trajectories of brain areas is a first step toward identifying different critical periods in the sensory cortices during which targeted sensory interventions may be provided.

In this study, to test the effects of PMA in preterm infants, we combined TEA data acquired at 3 T and pre-TEA data acquired at 1.5 T. As discussed previously, we attempted to address how ReHo, and by proxy cortical maturity, is affected by postnatal sensory experience by investigating the effect of PMA on ReHo. By including the pre-TEA scans, we examined this relationship over an extended course of preterm development. This is important because postnatal experience does not play an equal role across all developmental stages.[29,53] This does raise concerns regarding the effect of scanner strength on our results. However, despite the technical limitations that required two scanner strengths (see STAR Methods), examination of our partial dependence plots (Figure 3) shows a clear linear relationship between PMA and ReHo after accounting for the other variables in all three sensory ROIs. If scanner strength alone accounted for these differences, we would anticipate a stepwise difference between the two groups rather than the continuous relationship seen here. It is also possible that the 1.5 T scanner reduces the spatial specificity of the BOLD signal and inflates ReHo values. However, in this scenario, we would expect this phenomenon to reduce the effects presented in the manuscript. Still, we acknowledge that scanner strength may have affected our results in ways that we were unable to account for and is a technical limitation of the current work.

Finally, we demonstrated a significant negative connection between ReHo in the auditory cortex of preterm infants and MCHAT scores. Autism is a neurodevelopmental disorder that is often characterized by hypo- or hypersensitivity to sensory stimuli.[8] For instance, individuals with autism may have disproportionate responses, compared to neurotypical individuals, when exposed to mild auditory or tactile stimuli. Although prior work[65–67] has highlighted the role of long-range sensory cortex connectivity for conferring autism risk, we show that alteration of the local functional properties may play a role as well. Notably, autism may be mediated by noisier sensory processing due to imbalances in inhibition and excitation.[34,68–70] Such imbalances are a mark of cortical circuit immaturity and, like the results in the current study, can cause reduced ReHo as well. Overall, these data suggest that reduced ReHo may be a marker of increased risk of neurodevelopmental disability.

Limitations of the study

There are limitations to the current study. First, ReHo may be influenced by several confounding factors such as respiration and the cardiac cycle. It is possible that these factors may lead to differences among term and preterm infants but less clear how it affects the relationship among sensory cortices within individuals. It will be important for follow-up studies to adequately measure respiratory and cardiac activity to establish ReHo as a true marker of sensory cortex dysmaturity. Next, we were unable to tease apart the effects of postnatal sensory experience from PMA in the current work. Although we could attempt to do so by incorporating chronological age and PMA in the same model, such efforts are fraught due to the high correlation between these measures. Instead, future studies should try to explicitly control the level of sensory experience—for instance through sensory enrichment paradigms. Another limitation of the study is that it is unclear how the variations in the voxel sizes acquired across scans affects ReHo. This was done to accommodate different infant head sizes within the field of view. Ultimately, the TR was kept the same across all scans irrespective of the voxel size and we resampled all data to the same 3 mm isotropic grid to minimize these differences. Finally, our exploratory results examining the relationship between ReHo and future autism risk have a much smaller *n* than needed for generalizable brain-behavior relations[71] and thus should be interpreted cautiously. Furthermore, while the MCHAT score is commonly used to screen for autism risk, comorbidities with language or cognitive development, as is common in preterm infants, may affect the accuracy and specificity relative to autism diagnosis. We are currently expanding our neurodevelopmental dataset to test this and to confirm future autism spectrum diagnoses in our patients. This work will be crucial to support ReHo as an early reliable marker of autism as well as broader cognitive/language or social developmental delay(s).

In conclusion, our results suggest that preterm birth and PMA differently affect sensory cortices in preterm infants without structural brain injury. Local cortical circuits in primary somatosensory and auditory areas are particularly sensitive to preterm birth. This may reflect improper or atypical sensory experience during a critical developmental period. This altered local circuit activity in the auditory cortex may be a marker for increased risk of neurodevelopmental disability. In sum, this work advances our understanding of how experience-dependent and independent factors differentially shape the local functional properties of sensory cortices during early brain development.

STAR★METHODS

Detailed methods are provided in the online version of this paper and include the following:

- KEY RESOURCES TABLE
- RESOURCE AVAILABILITY
  - Lead contact

SUPPLEMENTAL INFORMATION

Supplemental information can be found online at https://doi.org/10.1016/j.isci.2024.109662.

ACKNOWLEDGMENTS

Support for this research was provided by the National Heart, Lung, and Blood Institute (RO1-HL116585-01), Eunice Kennedy Shriver National Institute of Child Health and Human Development (RO1-HD099393 and U54-HD090257), and the Canadian Institutes of Health Research (MOP-81116).

AUTHOR CONTRIBUTIONS

S.R.D. – conceptualization, methodology, software, formal analysis, writing – original draft, review and editing, and visualization. J.D.A.-C. – conceptualization, methodology, writing – review and editing, supervision, and project administration. K.M.C. – data curation and resources. K.K. – investigation and project administration. E.S. – data curation and resources. J.M. – investigation. S.B. – project administration and investigation. N.A. – conceptualization, methodology, writing – review and editing, supervision, project administration, and funding acquisition. C.L. – writing – review and editing, supervision, project administration, and funding acquisition.

DECLARATION OF INTERESTS

The authors declare no competing financial interests.

Received: September 7, 2023
Revised: January 23, 2024
Accepted: April 1, 2024
Published: April 4, 2024

REFERENCES

1. Reh, R.K., Dias, B.G., Nelson, C.A., Kaufer, D., Werker, J.F., Kolb, B., Levine, J.D., and Hensch, T.K. (2020). Critical period regulation across multiple timescales. Proc National Acad Sci *117*, 23242–23251. https://doi.org/10.1073/pnas.1820836117.
2. Werker, J.F., and Hensch, T.K. (2015). Critical Periods in Speech Perception: New Directions. Annu. Rev. Psychol. *66*, 173–196. https://doi.org/10.1146/annurev-psych-010814-015104.
3. Wiesel, T.N., and Hubel, D.H. (1965). Extent of Recovery From the Effects of Visual Deprivation in Kittens. J. Neurophysiol. *28*, 1060–1072. https://doi.org/10.1152/jn.1965.28.6.1060.
4. Hensch, T.K. (2005). Critical period plasticity in local cortical circuits. Nat. Rev. Neurosci. *6*, 877–888. https://doi.org/10.1038/nrn1787.
5. Huttenlocher, P.R., and Dabholkar, A.S. (1997). Regional differences in synaptogenesis in human cerebral cortex. J. Comp. Neurol. *387*, 167–178. https://doi.org/10.1002/(sici)1096-9861(19971020)387:2<167::aid-cne1>3.0.co;2-z.
6. Simpson, K.L., Weaver, K.J., de Villers-Sidani, E., Lu, J.Y.-F., Cai, Z., Pang, Y., Rodriguez-Porcel, F., Paul, I.A., Merzenich, M., and Lin, R.C.S. (2011). Perinatal antidepressant exposure alters cortical network function in rodents. Proc National Acad Sci *108*, 18465–18470. https://doi.org/10.1073/pnas.1109353108.
7. Weikum, W.M., Oberlander, T.F., Hensch, T.K., and Werker, J.F. (2012). Prenatal exposure to antidepressants and depressed maternal mood alter trajectory of infant speech perception. Proc National Acad Sci *109*, 17221–17227. https://doi.org/10.1073/pnas.1121263109.
8. Lord, C., Brugha, T.S., Charman, T., Cusack, J., Dumas, G., Frazier, T., Jones, E.J.H., Jones, R.M., Pickles, A., State, M.W., et al. (2020). Autism spectrum disorder. Nat. Rev. Dis. Primers *6*, 5. https://doi.org/10.1038/s41572-019-0138-4.
9. Galiana-Simal, A., Vela-Romero, M., Romero-Vela, V.M., Oliver-Tercero, N., García-Olmo, V., Benito-Castellanos, P.J., Muñoz-Martinez, V., and Beato-Fernandez, L. (2020). Sensory processing disorder: Key points of a frequent alteration in neurodevelopmental disorders. Cogent Medicine *7*, 1736829. https://doi.org/10.1080/2331205x.2020.1736829.
10. Rahkonen, P., Lano, A., Pesonen, A.K., Heinonen, K., Räikkönen, K., Vanhatalo, S., Autti, T., Valanne, L., Andersson, S., and Metsäranta, M. (2015). Atypical sensory processing is common in extremely low gestational age children. Acta Paediatr. *104*, 522–528. https://doi.org/10.1111/apa.12911.
11. Cabral, T.I., da Silva, L.G.P., Martinez, C.M.S., and Tudella, E. (2016). Analysis of sensory processing in preterm infants. Early Hum. Dev. *103*, 77–81. https://doi.org/10.1016/j.earlhumdev.2016.06.010.

12. Duerden, E.G., Mclean, M.A., Chau, C., Guo, T., Mackay, M., Chau, V., Synnes, A., Miller, S.P., and Grunau, R.E. (2022). Neonatal pain, thalamic development and sensory processing behaviour in children born very preterm. Early Hum. Dev. *170*, 105617. https://doi.org/10.1016/j.earlhumdev.2022.105617.
13. Smyser, C.D., Inder, T.E., Shimony, J.S., Hill, J.E., Degnan, A.J., Snyder, A.Z., and Neil, J.J. (2010). Longitudinal Analysis of Neural Network Development in Preterm Infants. Cereb. Cortex *20*, 2852–2862. https://doi.org/10.1093/cercor/bhq035.
14. Kwon, S.H., Scheinost, D., Vohr, B., Lacadie, C., Schneider, K., Dai, F., Sze, G., Constable, R.T., and Ment, L.R. (2016). Functional magnetic resonance connectivity studies in infants born preterm: suggestions of proximate and long-lasting changes in language organization. Dev. Med. Child Neurol. *58*, 28–34. https://doi.org/10.1111/dmcn.13043.
15. Doria, V., Beckmann, C.F., Arichi, T., Merchant, N., Groppo, M., Turkheimer, F.E., Counsell, S.J., Murgasova, M., Aljabar, P., Nunes, R.G., et al. (2010). Emergence of resting state networks in the preterm human brain. Proc National Acad Sci *107*, 20015–20020. https://doi.org/10.1073/pnas.1007921107.
16. Toulmin, H., Beckmann, C.F., O'Muircheartaigh, J., Ball, G., Nongena, P., Makropoulos, A., Ederies, A., Counsell, S.J., Kennea, N., Arichi, T., et al. (2015). Specialization and integration of functional thalamocortical connectivity in the human infant. Proc National Acad Sci *112*, 6485–6490. https://doi.org/10.1073/pnas.1422638112.
17. Smyser, C.D., Snyder, A.Z., Shimony, J.S., Mitra, A., Inder, T.E., and Neil, J.J. (2016). Resting-State Network Complexity and Magnitude Are Reduced in Prematurely Born Infants. Cereb. Cortex *26*, 322–333. https://doi.org/10.1093/cercor/bhu251.
18. Bouyssi-Kobar, M., De Asis-Cruz, J., Murnick, J., Chang, T., and Limperopoulos, C. (2019). Altered Functional Brain Network Integration, Segregation, and Modularity in Infants Born Very Preterm at Term-Equivalent Age. J. Pediatr. *213*, 13–21.e1. https://doi.org/10.1016/j.jpeds.2019.06.030.
19. Scheinost, D., Lacadie, C., Vohr, B.R., Schneider, K.C., Papademetris, X., Constable, R.T., and Ment, L.R. (2015). Cerebral Lateralization is Protective in the Very Prematurely Born. Cereb. Cortex *25*, 1858–1866. https://doi.org/10.1093/cercor/bht430.
20. Kwon, S.H., Scheinost, D., Lacadie, C., Sze, G., Schneider, K.C., Dai, F., Constable, R.T., and Ment, L.R. (2015). Adaptive mechanisms of developing brain: Cerebral lateralization in the prematurely-born. Neuroimage *108*, 144–150. https://doi.org/10.1016/j.neuroimage.2014.12.032.
21. Eyre, M., Fitzgibbon, S.P., Ciarrusta, J., Cordero-Grande, L., Price, A.N., Poppe, T., Schuh, A., Hughes, E., O'Keeffe, C., Brandon, J., et al. (2021). The Developing Human Connectome Project: typical and disrupted perinatal functional connectivity. Brain *144*, 2199–2213. https://doi.org/10.1093/brain/awab118.
22. Ball, G., Boardman, J.P., Aljabar, P., Pandit, A., Arichi, T., Merchant, N., Rueckert, D., Edwards, A.D., and Counsell, S.J. (2013). The influence of preterm birth on the developing thalamocortical connectome. Cortex *49*, 1711–1721. https://doi.org/10.1016/j.cortex.2012.07.006.
23. Dehaene, S., Cohen, L., Morais, J., and Kolinsky, R. (2015). Illiterate to literate: behavioural and cerebral changes induced by reading acquisition. Nat. Rev. Neurosci. *16*, 234–244. https://doi.org/10.1038/nrn3924.
24. Travis, K., Ford, K., and Jacobs, B. (2005). Regional Dendritic Variation in Neonatal Human Cortex: A Quantitative Golgi Study. Dev. Neurosci. *27*, 277–287. https://doi.org/10.1159/000086707.
25. Huttenlocher, P.R. (1990). Morphometric study of human cerebral cortex development. Neuropsychologia *28*, 517–527. https://doi.org/10.1016/0028-3932(90)90031-i.
26. Bourgeois, J.P., and Rakic, P. (1993). Changes of synaptic density in the primary visual cortex of the macaque monkey from fetal to adult stage. J. Neurosci. *13*, 2801–2820. https://doi.org/10.1523/jneurosci.13-07-02801.1993.
27. Bourgeois, J.P., Jastreboff, P.J., and Rakic, P. (1989). Synaptogenesis in visual cortex of normal and preterm monkeys: evidence for intrinsic regulation of synaptic overproduction. Proc National Acad Sci *86*, 4297–4301. https://doi.org/10.1073/pnas.86.11.4297.
28. Dimitrova, R., Pietsch, M., Ciarrusta, J., Fitzgibbon, S.P., Williams, L.Z.J., Christiaens, D., Cordero-Grande, L., Batalle, D., Makropoulos, A., Schuh, A., et al. (2021). Preterm birth alters the development of cortical microstructure and morphology at term-equivalent age. Neuroimage *243*, 118488. https://doi.org/10.1016/j.neuroimage.2021.118488.
29. Batalle, D., O'Muircheartaigh, J., Makropoulos, A., Kelly, C.J., Dimitrova, R., Hughes, E.J., Hajnal, J.V., Zhang, H., Alexander, D.C., Edwards, A.D., and Counsell, S.J. (2019). Different patterns of cortical maturation before and after 38 weeks gestational age demonstrated by diffusion MRI in vivo. Neuroimage *185*, 764–775. https://doi.org/10.1016/j.neuroimage.2018.05.046.
30. Jiang, L., and Zuo, X.-N. (2016). Regional Homogeneity. Neurosci *22*, 486–505. https://doi.org/10.1177/1073858415595004.
31. Zang, Y., Jiang, T., Lu, Y., He, Y., and Tian, L. (2004). Regional homogeneity approach to fMRI data analysis. Neuroimage *22*, 394–400. https://doi.org/10.1016/j.neuroimage.2003.12.030.
32. Zuo, X.-N., Xu, T., Jiang, L., Yang, Z., Cao, X.-Y., He, Y., Zang, Y.-F., Castellanos, F.X., and Milham, M.P. (2013). Toward reliable characterization of functional homogeneity in the human brain: Preprocessing, scan duration, imaging resolution and computational space. Neuroimage *65*, 374–386. https://doi.org/10.1016/j.neuroimage.2012.10.017.
33. Harrison, T.M., Maass, A., Adams, J.N., Du, R., Baker, S.L., and Jagust, W.J. (2019). Tau deposition is associated with functional isolation of the hippocampus in aging. Nat. Commun. *10*, 4900. https://doi.org/10.1038/s41467-019-12921-z.
34. Markicevic, M., Fulcher, B.D., Lewis, C., Helmchen, F., Rudin, M., Zerbi, V., and Wenderoth, N. (2020). Cortical Excitation:Inhibition Imbalance Causes Abnormal Brain Network Dynamics as Observed in Neurodevelopmental Disorders. Cereb. Cortex *30*, 4922–4937. https://doi.org/10.1093/cercor/bhaa084.
35. Li, Y., Booth, J.R., Peng, D., Zang, Y., Li, J., Yan, C., and Ding, G. (2013). Altered Intra- and Inter-Regional Synchronization of Superior Temporal Cortex in Deaf People. Cereb. Cortex *23*, 1988–1996. https://doi.org/10.1093/cercor/bhs185.
36. Liu, C., Liu, Y., Li, W., Wang, D., Jiang, T., Zhang, Y., and Yu, C. (2011). Increased regional homogeneity of blood oxygen level-dependent signals in occipital cortex of early blind individuals. Neuroreport *22*, 190–194. https://doi.org/10.1097/wnr.0b013e3283447c09.
37. Koyama, M.S., Ortiz-Mantilla, S., Roesler, C.P., Milham, M.P., and Benasich, A.A. (2017). A Modulatory Effect of Brief Passive Exposure to Non-linguistic Sounds on Intrinsic Functional Connectivity: Relevance to Cognitive Performance. Cereb. Cortex *27*, 5817–5830. https://doi.org/10.1093/cercor/bhx266.
38. Ciarrusta, J., Dimitrova, R., Batalle, D., O'Muircheartaigh, J., Cordero-Grande, L., Price, A., Hughes, E., Kangas, J., Perry, E., Javed, A., et al. (2020). Emerging functional connectivity differences in newborn infants vulnerable to autism spectrum disorders. Transl Psychiat *10*, 131. https://doi.org/10.1038/s41398-020-0805-y.
39. Sun, D., Guo, H., Womer, F.Y., Yang, J., Tang, J., Liu, J., Zhu, Y., Duan, J., Peng, Z., Wang, H., et al. (2021). Frontal-posterior functional imbalance and aberrant function developmental patterns in schizophrenia. Transl Psychiat *11*, 495. https://doi.org/10.1038/s41398-021-01617-y.
40. Larivière, S., de Wael, R.V., Hong, S.-J., Paquola, C., Tavakol, S., Lowe, A.J., Schrader, D.V., and Bernhardt, B.C. (2019). Multiscale Structure–Function Gradients in the Neonatal Connectome. Cereb Cortex *30*, 47–58. https://doi.org/10.1093/cercor/bhz069.
41. Toulmin, H., O'Muircheartaigh, J., Counsell, S.J., Falconer, S., Chew, A., Beckmann, C.F., and Edwards, A.D. (2021). Functional thalamocortical connectivity at term equivalent age and outcome at 2 years in infants born preterm. Cortex *135*, 17–29. https://doi.org/10.1016/j.cortex.2020.09.022.
42. Uhlhaas, P.J., Roux, F., Rodriguez, E., Rotarska-Jagiela, A., and Singer, W. (2010). Neural synchrony and the development of cortical networks. Trends Cogn. Sci. *14*, 72–80. https://doi.org/10.1016/j.tics.2009.12.002.
43. Khazipov, R., Minlebaev, M., and Valeeva, G. (2013). Early gamma oscillations. Neuroscience *250*, 240–252. https://doi.org/10.1016/j.neuroscience.2013.07.019.
44. Colonnese, M., and Khazipov, R. (2012). Spontaneous activity in developing sensory circuits: Implications for resting state fMRI. Neuroimage *62*, 2212–2221. https://doi.org/10.1016/j.neuroimage.2012.02.046.
45. Quast, K.B., Reh, R.K., Caiati, M.D., Kopell, N., McCarthy, M.M., and Hensch, T.K. (2023). Rapid synaptic and gamma rhythm signature of mouse critical period plasticity. Proc National Acad Sci *120*, e2123182120. https://doi.org/10.1073/pnas.2123182120.
46. Donahue, C.J., Glasser, M.F., Preuss, T.M., Rilling, J.K., and Van Essen, D.C. (2018). Quantitative assessment of prefrontal cortex in humans relative to nonhuman primates. Proc. Natl. Acad. Sci. *115*, E5183–E5192. https://doi.org/10.1073/pnas.1721653115.

47. Cruz-Rizzolo, R.J., De Lima, M.A.X., Ervolino, E., de Oliveira, J.A., and Casatti, C.A. (2011). Cyto-myelo- and chemoarchitecture of the prefrontal cortex of the Cebus monkey. BMC Neurosci. *12*, 6. https://doi.org/10.1186/1471-2202-12-6.
48. Mesulam, M. (2008). Representation, inference, and transcendent encoding in neurocognitive networks of the human brain. Ann. Neurol. *64*, 367–378. https://doi.org/10.1002/ana.21534.
49. Shaw, P., Kabani, N.J., Lerch, J.P., Eckstrand, K., Lenroot, R., Gogtay, N., Greenstein, D., Clasen, L., Evans, A., Rapoport, J.L., et al. (2008). Neurodevelopmental Trajectories of the Human Cerebral Cortex. J. Neurosci. *28*, 3586–3594. https://doi.org/10.1523/jneurosci.5309-07.2008.
50. Lordier, L., Meskaldji, D.-E., Grouiller, F., Pittet, M.P., Vollenweider, A., Vasung, L., Borradori-Tolsa, C., Lazeyras, F., Grandjean, D., Van De Ville, D., and Hüppi, P.S. (2019). Music in premature infants enhances high-level cognitive brain networks. Proc National Acad Sci *116*, 12103–12108. https://doi.org/10.1073/pnas.1817536116.
51. Lordier, L., Loukas, S., Grouiller, F., Vollenweider, A., Vasung, L., Meskaldij, D.-E., Lejeune, F., Pittet, M.P., Borradori-Tolsa, C., Lazeyras, F., et al. (2019). Music processing in preterm and full-term newborns: A psychophysiological interaction (PPI) approach in neonatal fMRI. Neuroimage *185*, 857–864. https://doi.org/10.1016/j.neuroimage.2018.03.078.
52. Pineda, R.G., Neil, J., Dierker, D., Smyser, C.D., Wallendorf, M., Kidokoro, H., Reynolds, L.C., Walker, S., Rogers, C., Mathur, A.M., et al. (2014). Alterations in Brain Structure and Neurodevelopmental Outcome in Preterm Infants Hospitalized in Different Neonatal Intensive Care Unit Environments. J. Pediatr. *164*, 52–60.e2. https://doi.org/10.1016/j.jpeds.2013.08.047.
53. Allievi, A.G., Arichi, T., Tusor, N., Kimpton, J., Arulkumaran, S., Counsell, S.J., Edwards, A.D., and Burdet, E. (2016). Maturation of Sensori-Motor Functional Responses in the Preterm Brain. Cereb. Cortex *26*, 402–413. https://doi.org/10.1093/cercor/bhv203.
54. Vinall, J., Grunau, R.E., Brant, R., Chau, V., Poskitt, K.J., Synnes, A.R., and Miller, S.P. (2013). Slower Postnatal Growth Is Associated with Delayed Cerebral Cortical Maturation in Preterm Newborns. Sci. Transl. Med. *5*, 168ra8. https://doi.org/10.1126/scitranslmed.3004666.
55. Dean, J.M., McClendon, E., Hansen, K., Azimi-Zonooz, A., Chen, K., Riddle, A., Gong, X., Sharifnia, E., Hagen, M., Ahmad, T., et al. (2013). Prenatal Cerebral Ischemia Disrupts MRI-Defined Cortical Microstructure Through Disturbances in Neuronal Arborization. Sci. Transl. Med. *5*, 168ra7. https://doi.org/10.1126/scitranslmed.3004669.
56. Ball, G., Pazderova, L., Chew, A., Tusor, N., Merchant, N., Arichi, T., Allsop, J.M., Cowan, F.M., Edwards, A.D., and Counsell, S.J. (2015). Thalamocortical Connectivity Predicts Cognition in Children Born Preterm. Cereb. Cortex *25*, 4310–4318. https://doi.org/10.1093/cercor/bhu331.
57. Smyser, C.D., Dosenbach, N.U.F., Smyser, T.A., Snyder, A.Z., Rogers, C.E., Inder, T.E., Schlaggar, B.L., and Neil, J.J. (2016). Prediction of brain maturity in infants using machine-learning algorithms. Neuroimage *136*, 1–9. https://doi.org/10.1016/j.neuroimage.2016.05.029.
58. De Asis-Cruz, J., Kapse, K., Basu, S.K., Said, M., Scheinost, D., Murnick, J., Chang, T., du Plessis, A., and Limperopoulos, C. (2020). Functional brain connectivity in ex utero premature infants compared to in utero fetuses. Neuroimage *219*, 117043. https://doi.org/10.1016/j.neuroimage.2020.117043.
59. Ricci, D., Cesarini, L., Romeo, D.M.M., Gallini, F., Serrao, F., Groppo, M., De Carli, A., Cota, F., Lepore, D., Molle, F., et al. (2008). Visual Function at 35 and 40 Weeks' Postmenstrual Age in Low-Risk Preterm Infants. Pediatrics *122*, e1193–e1198. https://doi.org/10.1542/peds.2008-1888.
60. Schwindt, E., Giordano, V., Rona, Z., Czaba-Hnizdo, C., Olischar, M., Waldhoer, T., Werther, T., Fuiko, R., Berger, A., and Klebermass-Schrehof, K. (2018). The impact of extrauterine life on visual maturation in extremely preterm born infants. Pediatr. Res. *84*, 403–410. https://doi.org/10.1038/s41390-018-0084-y.
61. Gee, D.G., Gabard-Durnam, L.J., Flannery, J., Goff, B., Humphreys, K.L., Telzer, E.H., Hare, T.A., Bookheimer, S.Y., and Tottenham, N. (2013). Early developmental emergence of human amygdala–prefrontal connectivity after maternal deprivation. Proc. Natl. Acad. Sci. USA *110*, 15638–15643. https://doi.org/10.1073/pnas.1307893110.
62. Witteveen, I.F., McCoy, E., Holsworth, T.D., Shen, C.Z., Chang, W., Nance, M.G., Belkowitz, A.R., Dougald, A., Puglia, M.H., and Ribic, A. (2023). Preterm birth accelerates the maturation of spontaneous and resting activity in the visual cortex. Frontiers Integr. Neurosci *17*, 1149159. https://doi.org/10.3389/fnint.2023.1149159.
63. Mowery, T.M., Kotak, V.C., and Sanes, D.H. (2016). The onset of visual experience gates auditory cortex critical periods. Nat. Commun. *7*, 10416. https://doi.org/10.1038/ncomms10416.
64. Henschke, J.U., Oelschlegel, A.M., Angenstein, F., Ohl, F.W., Goldschmidt, J., Kanold, P.O., and Budinger, E. (2018). Early sensory experience influences the development of multisensory thalamocortical and intracortical connections of primary sensory cortices. Brain Struct. Funct. *223*, 1165–1190. https://doi.org/10.1007/s00429-017-1549-1.
65. Plitt, M., Barnes, K.A., Wallace, G.L., Kenworthy, L., and Martin, A. (2015). Resting-state functional connectivity predicts longitudinal change in autistic traits and adaptive functioning in autism. Proc National Acad Sci *112*, E6699–E6706. https://doi.org/10.1073/pnas.1510098112.
66. King, J.B., Prigge, M.B.D., King, C.K., Morgan, J., Weathersby, F., Fox, J.C., Dean, D.C., Freeman, A., Villaruz, J.A.M., Kane, K.L., et al. (2019). Generalizability and reproducibility of functional connectivity in autism. Mol. Autism. *10*, 27. https://doi.org/10.1186/s13229-019-0273-5.
67. O'Reilly, C., Lewis, J.D., and Elsabbagh, M. (2017). Is functional brain connectivity atypical in autism? A systematic review of EEG and MEG studies. PLoS One *12*, e0175870. https://doi.org/10.1371/journal.pone.0175870.
68. Rosenberg, A., Patterson, J.S., and Angelaki, D.E. (2015). A computational perspective on autism. Proc National Acad Sci *112*, 9158–9165. https://doi.org/10.1073/pnas.1510583112.
69. Rubenstein, J.L.R., and Merzenich, M.M. (2003). Model of autism: increased ratio of excitation/inhibition in key neural systems. Genes Brain Behav. *2*, 255–267. https://doi.org/10.1034/j.1601-183x.2003.00037.x.
70. Masuda, F., Nakajima, S., Miyazaki, T., Yoshida, K., Tsugawa, S., Wada, M., Ogyu, K., Croarkin, P.E., Blumberger, D.M., Daskalakis, Z.J., et al. (2019). Motor cortex excitability and inhibitory imbalance in autism spectrum disorder assessed with transcranial magnetic stimulation: a systematic review. Transl Psychiat *9*, 110. https://doi.org/10.1038/s41398-019-0444-3.
71. Marek, S., Tervo-Clemmens, B., Calabro, F.J., Montez, D.F., Kay, B.P., Hatoum, A.S., Donohue, M.R., Foran, W., Miller, R.L., Hendrickson, T.J., et al. (2022). Reproducible brain-wide association studies require thousands of individuals. Nature *603*, 654–660. https://doi.org/10.1038/s41586-022-04492-9.
72. Robins, D.L., Casagrande, K., Barton, M., Chen, C.-M.A., Dumont-Mathieu, T., and Fein, D. (2014). Validation of the Modified Checklist for Autism in Toddlers, Revised With Follow-up (M-CHAT-R/F). Pediatrics *133*, 37–45. https://doi.org/10.1542/peds.2013-1813.
73. Cox, R.W. (1996). AFNI: Software for Analysis and Visualization of Functional Magnetic Resonance Neuroimages. Comput. Biomed. Res. *29*, 162–173. https://doi.org/10.1006/cbmr.1996.0014.
74. Hallquist, M.N., Hwang, K., and Luna, B. (2013). The nuisance of nuisance regression: Spectral misspecification in a common approach to resting-state fMRI preprocessing reintroduces noise and obscures functional connectivity. Neuroimage *82*, 208–225. https://doi.org/10.1016/j.neuroimage.2013.05.116.
75. Behzadi, Y., Restom, K., Liau, J., and Liu, T.T. (2007). A component based noise correction method (CompCor) for BOLD and perfusion based fMRI. Neuroimage *37*, 90–101. https://doi.org/10.1016/j.neuroimage.2007.04.042.
76. Reynolds, R.C., Taylor, P.A., and Glen, D.R. (2022). Quality control practices in FMRI analysis: Philosophy, methods and examples using AFNI. Front. Neurosci. *16*, 1073800. https://doi.org/10.3389/fnins.2022.1073800.
77. Taylor, P.A., and Saad, Z.S. (2013). FATCAT: (An Efficient) Functional And Tractographic Connectivity Analysis Toolbox. Brain Connect. *3*, 523–535. https://doi.org/10.1089/brain.2013.0154.
78. Zuo, X.-N., Di Martino, A., Kelly, C., Shehzad, Z.E., Gee, D.G., Klein, D.F., Castellanos, F.X., Biswal, B.B., and Milham, M.P. (2010). The oscillating brain: Complex and reliable. Neuroimage *49*, 1432–1445. https://doi.org/10.1016/j.neuroimage.2009.09.037.
79. Shi, F., Yap, P.-T., Wu, G., Jia, H., Gilmore, J.H., Lin, W., and Shen, D. (2011). Infant Brain Atlases from Neonates to 1- and 2-Year-Olds. PLoS One *6*, e18746. https://doi.org/10.1371/journal.pone.0018746.
80. Damera, S.R., Chang, L., Nikolov, P.P., Mattei, J.A., Banerjee, S., Glezer, L.S., Cox, P.H., Jiang, X., Rauschecker, J.P., and Riesenhuber, M. (2023). Evidence for a Spoken Word Lexicon in the Auditory Ventral Stream. Neurobiology Lang. *4*, 1–40. https://doi.org/10.1162/nol_a_00108.
81. Glezer, L.S., Kim, J., Rule, J., Jiang, X., and Riesenhuber, M. (2015). Adding Words to the

Brain's Visual Dictionary: Novel Word Learning Selectively Sharpens Orthographic Representations in the VWFA. J. Neurosci. *35*, 4965–4972. https://doi.org/10.1523/jneurosci.4031-14.2015.

82. Murty, N.A.R., Teng, S., Beeler, D., Mynick, A., Oliva, A., and Kanwisher, N. (2020). Visual experience is not necessary for the development of face-selectivity in the lateral fusiform gyrus. Proc National Acad Sci *202004607*. https://doi.org/10.1073/pnas.2004607117.
83. Boring, M.J., Silson, E.H., Ward, M.J., Richardson, R.M., Fiez, J.A., Baker, C.I., and Ghuman, A.S. (2021). Multiple Adjoining Word- and Face-Selective Regions in Ventral Temporal Cortex Exhibit Distinct Dynamics. J. Neurosci. *41*, 6314–6327. https://doi.org/10.1523/jneurosci.3234-20.2021.
84. Bates, D., Mächler, M., Bolker, B., and Walker, S. (2015). Fitting Linear Mixed-Effects Models Using lme4. J. Stat. Softw. *67*. https://doi.org/10.18637/jss.v067.i01.
85. Oosterhof, N.N., Connolly, A.C., and Haxby, J.V. (2016). CoSMoMVPA: Multi-Modal Multivariate Pattern Analysis of Neuroimaging Data in Matlab/GNU Octave. Front. Neuroinform. *10*, 27. https://doi.org/10.3389/fninf.2016.00027.

STAR★METHODS

KEY RESOURCES TABLE

REAGENT or RESOURCE	SOURCE	IDENTIFIER
Software and algorithms		
AFNI	Cox et al.,[73]	https://doi.org/10.1006/cbmr.1996.0014
MATLAB 2020b	The MathWorks Inc.	https://www.mathworks.com/
R	R Core Team	https://www.r-project.org/
CosmoMVPA	Oosterhof et al.,[85]	https://doi.org/10.3389/fninf.2016.00027
Paper Code	This Paper	https://doi.org/10.5281/zenodo.10818502

RESOURCE AVAILABILITY

Lead contact

Further information and requests for resources should be directed to and will be fulfilled by the lead contact, Catherine Limperopoulos (climpero@childrensnational.org).

Materials availability

This study did not generate new unique reagents.

Data and code availability

- The data that support the findings of this study are available from the lead contact, Catherine Limperopoulos, upon reasonable request.
- All original code has been deposited at https://github.com/srd49/DBI/releases/tag/iscience and is publicly available as of the date of publication. DOIs are listed in the key resources table.
- Any additional information required to reanalyze the data reported in this paper is available from the lead contact upon request.

EXPERIMENTAL MODEL AND STUDY PARTICIPANT DETAILS

Participants

Subjects were recruited from the Neonatal Intensive Care Units (NICU) at Children's National Hospital (CNH, Washington, DC). All infants were prospectively recruited as part of a larger longitudinal observational studies investigating neurodevelopment in preterm infants. Term infants used as healthy controls were not recruited from NICU, and the study was approved by the institutional review board of CNH and written informed consent was obtained from parents of study participants. Exclusion criteria included chromosomal anomalies, dysmorphic features, congenital brain malformations, central nervous system infection, and metabolic disorders.

All MRI studies were reviewed by a single pediatric neuroradiologist (J.M.) and analyzed using the Kidokoro score to assess for brain injury.[52] Kidokoro scores ≥ 8 are indicative of moderate-to-severe global brain injury and subsequently excluded. Similarly, MRI acquisitions with significant motion (see below) yielding less than 5 min of usable resting-state data also were excluded. In total, we analyzed data from 86 term-born infants and 133 preterm infants. 109 of those preterm infants were scanned after term equivalent age (TEA; ≥ 37 weeks) weeks postmenstrual age (PMA) and 57 were scanned before TEA (Table 1).

Clinical variables

Clinical data were collected for preterm infants during their NICU stay. The effects of several common co-morbidities in preterm infants known to alter typical brain development also were examined in the current study. These included diagnosis of necrotizing enterocolitis (NEC), bronchopulmonary dysplasia (BPD), and patent ductus arteriosus (PDA). In addition to these measures, we also record biologic sex at birth, birth weight, if prenatal steroids (PNS) were given, PMA of preterm infants as their birth gestational age plus their chronological age at the time of MRI, and Modified Checklist for Autism in Toddlers (MCHAT)[72] scores collected at a neurodevelopmental follow-up visit at 18-month Table S1 summarizes the clinical characteristics of our study cohorts. We specifically excluded infants that were either small for gestational age (SGA) or large for gestational age (LGA), so that birth weight and GA at Birth are highly correlated ($r = 0.79$) – thus birth weight was excluded from the regression analyses discussed below.

METHOD DETAILS

Functional MRI data acquisition

All term infants were scanned on a 3T GE scanner. Preterm infants were scanned using a 1.5T GE scanner prior to TEA and a 3T scanner after TEA. A 1.5T scanner was used for scans prior to TEA because preterm infants at those ages required active thermoregulation and were imaged using an MR compatible incubator that was specific to the 1.5T scanner. By term, infants are much more stable to undergo imaging without the additional thermoregulation and thus were able to image using the 3T scanner. To facilitate sleep and minimize in-scanner movement, infants were fed, swaddled in a warm blanket, and immobilized using an infant vacuum pillow. To protect their hearing from scanner noise, they wore silicone earplugs and adhesive earmuffs.

At TEA infants were scanned using a 3 Tesla MRI scanner (Discovery MR750, General Electric Medical, Systems-Waukesha, WI) with an 8-channel receiver head coil. Anatomical T2-weighted fast spin echo (3D Cube) data were obtained in both full-term and preterm infants with a mean voxel size = 0.625 × 1 × 0.625 mm^3 [range: 0.2539 × 1.0 × 0.2539–0.7301 × 1.0 × 0.7301 mm^3]. Resting-state data, in full-term and preterm infants at TEA, were collected using a T2*-weighted gradient-echo planar imaging (EPI) sequence: TR = 2000 ms, TE = 35 ms, mean voxel size = 2.954 × 2.954 × 3.078 mm^3 [range: 1.875 × 1.875 × 3–3.125 × 3.125 × 3 mm^3], flip angle = 60°, slice number = 29 to 41, number of volumes = 200–300.

Prior to TEA, preterm infants were scanned after being medically cleared by the attending neonatologist using an MRI compatible incubator (LMT Medical System GmbH, Luebeck, Germany). These scans were performed on a 1.5 Tesla MRI scanner (Discovery MR450, General Electric Medical, Systems-Waukesha, WI) with a 1-channel receiver head coil. Anatomical 2mm sagittal, coronal, and axial single-shot fast spin echo (SSFSE) T2 weighted sequences (TR = 1100 ms, TE = 160 ms, FOV = 12, acquisition matrix = 192 × 128 mm3) were acquired. Resting-state data were collected using a T2*-weighted gradient-echo planar imaging (EPI) sequence: TR = 2000 ms, TE = 35 ms, mean voxel size = 2.430 × 2.425 × 4.125 mm^3 [range: 2.348 × 2.348 × 4–3.125 × 3.125 × 5 mm^3], flip angle = 60°, slice number = 20 to 33, number of volumes = 150–300.

Functional MRI data pre-processing

Image preprocessing was performed using AFNI[73] and custom MATLAB scripts. First within volume motion correction was performed on EPI data and then anatomical and EPI volumes were moved to the same space by aligning their centers. Then the first 4 acquisitions of each run were discarded to allow for T1 stabilization. Data was further preprocessed by 1) applying slice-time correction, 2) despiking EPI images to mitigate the effect of BOLD signal outliers, 3) applying bias-field correction, 4) realigning all EPI images to the volume to the base image (i.e., the image with the least number of outliers), 5) resampling all EPI images to a 3mm isotropic grid, 6) co-registering the base image to the anatomical scan, 7) segmenting anatomical images to produce gray matter (GM), white matter (WM), and cerebrospinal fluid (CSF) tissue masks, and 8) non-linear normalization of all images including tissue masks to age-specific templates. Transformations in steps 4, 6, and 8 were applied simultaneously to EPI BOLD data. The resulting resting state data was then intensity scaled to a global mode of 1000 and then bandpass filtered between 0.009 Hz and 0.08 Hz.[74] Data were then cleaned by removing the effect of tissue and motion regressors. Tissue regressors were derived from the eroded and localized WM and the first 5 principal components of the averaged CSF signal.[75] Motion regressors included linearly demeaned translational and rotational head motion parameters (generated in step 4), their temporal derivatives, and quadratic terms. Furthermore, the effects of high-motion volumes were accounted for by including a regressor marking volumes to be censored from the analysis. These EPI volumes were those that either exhibited framewise displacement (Euclidean Norm) > 0.2 mm or had >10% BOLD signal intensity outlier voxels as determined during despiking.[76] Censoring the data during regression rather than at an earlier step allows us to minimize the effect of high-motion volumes while preserving temporal dependencies in the data.

Computing regional homogeneity

Local regional homogeneity (ReHo)[30,31] was computed in standard space by using the AFNI sub-routine *3dReHo*.[77] Briefly, this function computes the Kendal Coefficient of Concordance between the BOLD time-series of a given voxel and its *n* closes neighbors. Here, the 27 closest neighbors corresponding to adjacent faces, edges, and nodes was used. ReHo values were then normalized by subtracting the mean of all non-zero voxels[78] to produce the final ReHo maps for each subject.

Defining sensory regions of interest (ROIs)

To test the distribution of ReHo, we first used a one-sample two-tailed t-test to identify voxels where ReHo was significantly greater than 0 at a voxel-wise threshold of $p \leq 0.001$ across all term and preterm infant scans acquired at TEA. To define sensory ROIs, we first masked this map by the sensory parcels in the infant neonatal AAL atlas.[79] Specifically, the left and right postcentral gyrus, calcarine cortex, and Heschl's as well as superior temporal gyrus parcels were used to define the somatosensory, visual, and auditory ROIs respectively. Two parcels (i.e., Heschl's and superior temporal gyrus) were used to define the auditory ROI to better equate the total mask volume across the sensory ROIs. We then iteratively threshold-ed the following map to generate ROIs of ~20 voxels each. Of note, 20 voxels (~540mm^3) was chosen to be similar to ROI volumes used in adult fMRI studies[80–83] which can range from ~200 to 500mm^3. Although ROIs containing a larger number of voxels could be used, we believe this would limit the interpretability of our results given the significantly smaller brain volumes of infants compared to adults. For the remaining analysis ReHo values were averaged within each sensory ROI for every subject.

Fitting regression models to ReHo in sensory cortex

Several linear regression and mixed effects models were used to test the effect of variables of interest on ReHo in the sensory cortices. These models were fit using the *lm* and *lmer*[84] functions in *R*. Mixed-effects models were used whenever repeat observations for the same subjects were included. In these models, *PretermBirth*, *Sex*, and *ClinicalCovariates* were categorical variables while *PMA*, *Motion*, and *MCHAT*, were continuous variables. The clinical covariates included diagnosis of NEC, BPD, PDA were made, and if prenatal steroids were received and were coded as binary variables. *Motion* was defined as the Euclidean norm of the movement between each volume acquired. We first tested the effect of preterm birth on ReHo at TEA using the following linear regression model:

$$ReHo \sim PretermBirth + PMA + Sex + Motion \quad \text{(Equation 1)}$$

We also explicitly tested if the effect of preterm birth differentially affected ReHo in the sensory cortices using the following linear mixed-effects model:

$$ReHo \sim PretermBirth * ROI + PMA + Sex + Motion + (1|Subject) \quad \text{(Equation 2)}$$

We then examined the developmental trajectory of ReHo in preterm infants by testing the effects of birth GA and PMA in preterm infants scanned before and after TEA (37 weeks PMA) using the following linear mixed-effects model:

$$ReHo \sim BirthGA + PMA + Sex + Motion + ClinicalCovaraiates + (1|Subject) \quad \text{(Equation 3)}$$

Here, PMA served as a proxy for postnatal sensory experience, which varies based on the degree of prematurity and/or duration of extrauterine exposure. By including the pre-TEA scans, we can examine this relationship over an extended course of preterm development.

We further tested if PMA differentially affected ReHo in the sensory cortices of preterm infants using the following linear mixed-effects model:

$$ReHo \sim BirthGA + PMA * ROI + Sex + Motion + ClinicalCovariates + (1|Subject) \quad \text{(Equation 4)}$$

Spatial specificity of the effect of preterm birth

We tested the spatial specificity of the effect on preterm birth on sensory cortices by comparing it against a control region – non-primary frontal cortex. To do so, we first built a mask of frontal cortical areas (Figure S2A) by masking areas with a significant positive ReHo (Figure 1A) and regions in the AAL atlas belonging to: superior, middle, inferior, and orbito-frontal gyri, insula, anterior, middle, and posterior cingulate. We then computed the average ReHo in searchlights of 20 voxels (the same size as our sensory ROIs) centered on each voxel within the mask and fit Equation 1 to estimate the effect size of preterm birth across the frontal cortex. Searchlights were created using CoSMoMVPA.[85] Next, we compared the distribution of effect sizes across frontal cortex to the effect sizes in each of our three sensory ROIs (Figure S2B).

Exploring the association between ReHo and MCHAT

We performed an exploratory analysis to test if ReHo at TEA was associated with future risk of autism in preterm infants for whom MCHAT scores were recorded at their 18-month neurodevelopmental follow-up visit. Given that we only had developmental follow-up data for 26 of our subjects, we optimized our sensitivity by using a backward model selection approach to identify the most parsimonious model that fit our data. To do so, we started with the full model:

$$MCHAT \sim BirthGA + PMA + Sex + Motion + ClinicalCovariates$$

Then iteratively reduced the model using the *step* function in *R*. This yielded the model:

$$MCHAT \sim PMA + NEC + BPD$$

We then added ReHo to this model to get our final model:

$$MCHAT \sim ReHo + PMA + NEC + BPD \quad \text{(Equation 5)}$$

Equations 1, 3, and 5 were fit separately for each ROI while Equations 2 and 4 were fit to data pooled across ROIs. Furthermore, Equations 1 and 2 used data from preterm and term infants at TEA, Equations 3 and 4 used data from the same preterm infants analyzed in the prior models as well as data from preterm infants scanned before TEA, and finally Equation 5 only used data from preterm infants scanned after TEA. Of note, some infants (n = 32) were scanned before and after TEA.

QUANTIFICATION AND STATISTICAL ANALYSIS

For Equations 1 and 3, the p-values for each factor (e.g., *PretermBirth*) were Hommel corrected for multiple comparisons across ROIs. Hommel corrected p-values (p_{HC}) are reported throughout the text, but uncorrected p-values are reported in the tables.

For Equation 2, we conducted the following 3 post-hoc tests: $PretermBirth_{Visual}$ vs. $PretermBirth_{Auditory}$, $PretermBirth_{Visual}$ vs. $PretermBirth_{Somatosensory}$, and $PretermBirth_{Somatosensory}$ vs. $PretermBirth_{Auditory}$. Similarly for Equation 4 we conducted the following 3 post-hoc tests: PMA_{Visual} vs. $PMA_{Auditory}$, PMA_{Visual} vs. $PMA_{Somatosensory}$, and $PMA_{Somatosensory}$ vs. $PMA_{Auditory}$. For each model, *p*-values were again corrected using Hommel correction across the three comparisons. These tests and corresponding *p*-value corrections were performed using the *emmeans* package in *R*.

Finally, given that Equation 5 was an exploratory analysis, no statical correction was performed.